Catalysis Science & Technology

Accepted Manuscript

ROYAL SOCIETY OF CHEMISTRY

www.rsc.org/catalysis

Catalysis Science & Technology

Catalysis Science & Technology

Dynamic Article Links ►

Cite this: DOI: 10.1039/c0xx00000x

www.rsc.org/xxxxxx

COMMUNICATION

Multi-scale promoting effects of lead for palladium catalyzed aerobic oxidative coupling of methylacrolein with methanol†

Junxing Han,[a] Suojiang Zhang,*[a] Yuchao Li[a,b] and Ruiyi Yan[a]

Received (in XXX, XXX) Xth XXXXXXXXX 20XX, Accepted Xth XXXXXXXXX 20XX

DOI: 10.1039/b000000x

A highly efficient Pd_2Pb_8/Alumina catalyst was prepared, which provided the highest turnover number (TON) of 302 for aerobic oxidative coupling of methylacrolein with methanol. The enhanced catalytic efficiency could be attributed to multi-scale (micron, nano and atom-scales) promoting effects of pre-loaded Pb species.

Oxidative coupling of aldehydes with methanol provides a highly efficient approach to directly produce methyl esters without the participation of carboxylic acids or carboxylic acid derivatives.[1] Among them, aerobic oxidative coupling of methylacrolein with methanol offers a sustainable and environmentally benign alternative to the traditional acetone cyanohydrin (ACH) method in the production of methyl methacrylate (MMA), an important monomer for polymers with a production capacity of 3 millions of tons in 2010.[2] The aerobic oxidative coupling reaction starts from methylacrolein, methanol and oxygen, avoids the utilization of toxic and corrosive HCN and H_2SO_4, and generates water as the only by-product (Scheme 1). Hence, much effort has been devoted to the novel process.[3] Up to now, Pd, Au and Co-based catalysts have been developed and identified as effective catalysts for aerobic oxidative coupling reactions.[4]

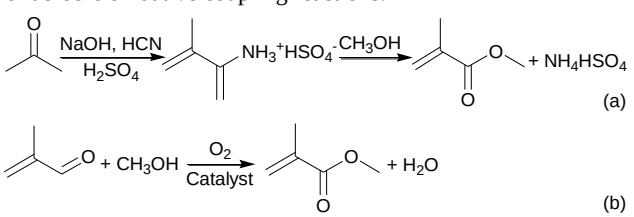

Scheme 1 Synthetic methods for MMA: (a) ACH method and (b) aerobic oxidative coupling of methylacrolein with methanol.

For Au and Co-based catalysts, long reaction time and much excessive methanol are needed to maintain high aldehyde conversion and product selectivity. Methylacrolein is an active substrate and prone to polymerization, decarbonylation and hydrogenation. Long reaction time may result in the generation of by-products and excessive methanol consumes much energy in subsequent product separation process. These problems could be solved by using Pd-based catalysts. Diao and co-workers reported a Pd-Pb bimetallic catalyst, over which aerobic oxidative coupling of methylacrolein with methanol could be completed in 2 h with a methanol/aldehye molar ratio of 8/1.[5] However, monometallic Pd catalysts could not meet the requirements due to low product selectivity.[6a] After doping Pb, prepared Pd-Pb bimetallic catalysts offered enhanced catalytic performance and a turnover number (TON), defined as the total number of product moles formed per mole of Pd catalyst, of 61 could be obtained.[6b] To date, the exact reason for the amazingly promoting effects of Pb remains unclear and the catalytic efficiency of Pd should be further improved due to its high cost and limited availability. Herein, we report a highly efficient Pd-Pb bimetallic catalyst, which provides a TON of 302, the highest efficiency reported, for the aerobic oxidative coupling of methylacrolein with methanol. The enhanced catalytic efficiency could be attributed to multi-scale promoting effects of pre-loaded Pb species.

Pd_mPb_n/Alumina catalysts (m and n represent the theoretical Pd and Pb loadings) were prepared by a stepwise method. Pb species were firstly deposited onto alumina by the wet impregnation method using $Pb(NO_3)_2$ as the precursor. After drying and calcination, Pb_n/Alumina composite supporters with variety of Pb loadings were obtained. Then, Pd was introduced by immersing Pb_n/Alumina into a Na_2PdCl_4 solution. After reduction with hydrazine at 90 ℃, Pd_mPb_n/Alumina bimetallic catalysts were acquired. Compositions of prepared Pd-Pb catalysts were listed in Table 1. It could be seen that actual ratios of Pb to Pd measured by the inductively coupled plasma-atomic emission spectroscopy (ICP-AES) are very close to the theoretical values.

Catalytic performance of prepared Pd_mPb_n/Alumina catalysts for aerobic oxidative coupling of methylacrolein with methanol was screened and the results were summarized in Table 1. Consistent with the reported work,[6a] monometallic Pd catalyst showed poor performance for the oxidative coupling reaction and the MMA selectivity was only 47% (Table 1, entry 1). By-products mainly include isobutyraldehyde (**a**), methyl isobutyrate (**b**), propylene (**c**), 1,1-dimethoxy-2-methylpropylene (**d**), methally alcohol (**e**), methacrylic acid (**f**), methacrylic anhydride (**g**) and isobutenyl methacrylate (**h**) (Scheme S1, ESI†). After doping Pb, catalytic performance was greatly improved. When Pb content increased to 8 wt%, Pd_2Pb_8/Alumina provided the best performance with a methylacrolein conversion of 82% and a MMA selectivity of 84% (Table 1, entry 5). Meanwhile, main by-product yields of **c**, **g** and **h** dropped from 2.5, 1.2 and 18.9% to 0.1, 0.5 and 3.4%, respectively. The calculated TON for

Table 1 Aerobic oxidative coupling of aldehydes with methanol over different catalysts[a]

Entry	Catalyst	Composition (%)			Conv. (%)	Sel. (%)
		Pd	Pb	Pb/Pd		
1	Pd_2/Alumina	1.60	0.00	0.00	79	47
2	Pd_2Pb_1/Alumina	1.52	0.81	0.53	77	50
3	Pd_2Pb_2/Alumina	1.39	1.44	1.04	70	62
4	Pd_2Pb_5/Alumina	1.58	3.74	2.37	78	78
5	Pd_2Pb_8/Alumina	1.78	6.29	3.53	82	84
6	Pd_2Pb_{10}/Alumina	1.39	6.70	4.82	78	80
7	Pd_2Pb_{20}/Alumina	1.33	9.78	7.35	30	50
8	Pb_8/Alumina	0.00	5.87		26	2
9	$Pd_{0.5}Pb_8$/Alumina	0.39	5.99	15.36	19	47
10	Pd_1Pb_8/Alumina	0.81	6.13	7.58	33	53
11	$Pd_{2.5}Pb_8$/Alumina	1.98	6.30	3.18	85	88
12[b]	$Pd_5Pb_5Mg_2$/Alumina	4.81	4.80	1.00	84	78
13[c]	Pd_2Pb_8/Alumina	1.78	6.29	3.53	96	95
14[d]	Pd_2Pb_8/Alumina	1.78	6.29	3.53	88	83
15[e]	Pd_2Pb_8/Alumina	1.78	6.29	3.53	71	92
16[f]	Pd_2Pb_8/Alumina	1.78	6.29	3.53	100	85
17[g]	Pd_2Pb_8/Alumina	1.78	6.29	3.53	100	95

[a] Reaction conditions: catalyst (2.5 g), methylacrolein (0.18 mol), methanol (1.44 mol), $Mg(OH)_2$ (0.15 g), 0.3 MPa O_2, 80℃, 2 h. [b] The catalyst was prepared according to the traditional method.[5] [c] Similar to entry a with 0.09 mol methylacrolein. [d] Reaction conditions: catalyst (0.75 g), isobutyraldehyde (0.04 mol), methanol (0.64 mol), $Mg(OH)_2$ (0.05 g), 0.3 MPa O_2, 60℃, 7 h. [e] Similar to entry d with 0.04 mol benzaldehyde. [f] Reaction conditions: catalyst (0.2 g), 4-chlorobenzaldehyde (0.0036 mol), methanol (0.64 mol), K_2CO_3 (0.1 g), 0.3 MPa O_2, 80℃, 8 h. [g] Similar to entry f with 0.0036 mol 4-methoxybenzaldehyde.

Pd_2Pb_8/Alumina was as high as 302, the highest number reported. Further increasing Pb loadings inhibited the catalytic efficiency (Table 1, entries 6 and 7). Hence, the optimal Pb content of 8 wt% was selected for further investigations.

Monometallic Pb catalyst was inactive and poorly selective for the oxidative coupling of methylacrolein with methanol (Table 1, entry 8). With the increment of Pd loadings, methylacrolein conversion and MMA selectivity improved dramatically (Table 1, entries 5 and 9-11), revealing that Pd provides active sites for the oxidative coupling reaction. When Pd content increased to 2%, the catalytic efficiency of Pd_2Pb_8/Alumina matched that of $Pd_5Pb_5Mg_2$/Alumina prepared with the reported method.[5] Considering Pd loadings, the catalytic efficiency of Pd_2Pb_8/Alumina was approximately 3-fold that of $Pd_5Pb_5Mg_2$/Alumina. Compared with the reported method, in which Pd precursors were firstly loaded onto the carriers, modifications made in the present work mainly include: (1) the Pb promoter was firstly loaded onto the carriers; (2) the content of Pb was elevated to 8 wt%. Therefore, we speculate that the amazingly improved catalytic efficiency of Pd_2Pb_8/Alumina might originate from promoting effects of preloaded Pb species.

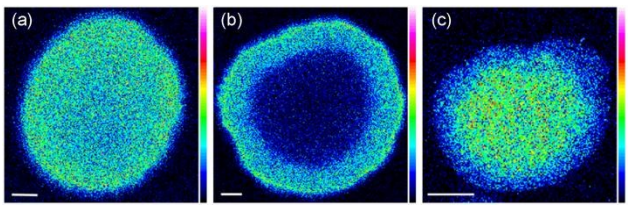

Fig. 1 X-ray microprobe mapping of Pd at the cross section of (a) Pd_2/Alumina, (b) Pd_2Pb_8/Alumina and (c) $Pd_5Pb_5Mg_2$/Alumina. The scale bars represent 20 μm.

First of all, X-ray microprobe technique was used to analyze the distribution of Pd in three typical catalysts. As shown in Fig. 1, uniform Pd distribution was obtained on monometallic Pd_2/Alumina and bimetallic $Pd_5Pb_5Mg_2$/Alumina (Fig. 1, a and c), both of which were prepared with the reported method, while an egg-shell structured Pd distribution with a depth of 20 μm was observed on Pd_2Pb_8/Alumina (Fig. 1, b), suggesting that pre-loaded Pb species facilitate the confinement of Pd precursor in the egg-shell region. Pre-loaded Pb species might be PbO originated from the decomposition of $Pb(NO_3)_2$ at 550 ℃,[7] though no diffraction peaks ascribed to PbO was detected in XRD measurements (Fig. S1, ESI†). CO_2 chemisorption experiments manifested that after loading 8 wt% of Pb onto alumina, CO_2 desorption temperatures increased by 50 ℃ with the CO_2 desorption amount increased from 7.13 to 16.65 μmol g^{-1} (Fig. S2 and Table S1, ESI †), revealing that pre-loaded Pb species enhanced the basic strength and increased basic site amounts of alumina carriers. Improved alkalinity of Pb_8/Alumina promotes the hydrolysis of $[PdCl_4]^{2-}$ precursors and strengthens the interaction of $[PdCl_x(OH)_{4-x}]^{2-}$ species with the positively charged alumina surface.[8] As a result, Pd precursors were confined in a region near the outer surface of alumina microspheres and an egg-shell structured Pd distribution formed. Pd provides active sites for the oxidative coupling reaction. However, on the uniformly dispersed catalysts such as Pd_2/Alumina and $Pd_5Pb_5Mg_2$/Alumina, active sites located in the inner micropores could not be used effectively due to steric hindrance and transfer resistance, which decreased the catalytic efficiency of the precious metal Pd. This problem was solved by confining active sites in the egg-shell region by pre-loading Pb. Therefore, from the micron-scale viewpoint, pre-loaded Pb species promote the confinement of Pd in the egg-shell region and improve the formation of more accessible active sites.

Fig. 2 shows TEM and HRTEM images of three representative catalysts. For monometallic Pd_2/Alumina, the *d*-spacing of 0.22 nm corresponded to the Pd (111) lattice (Fig. 2, d). After doping Pb, the *d*-spacing increased to 0.23 nm (Fig. 2, e and f), corresponding to the bimetallic Pd_3Pb (111) lattice.[5] In XRD patterns, the diffraction peak of Pd (111) lattice shifted from 40.2 ° to 38.6° after doping Pb (Fig. S3, ESI†), indicating the expansion

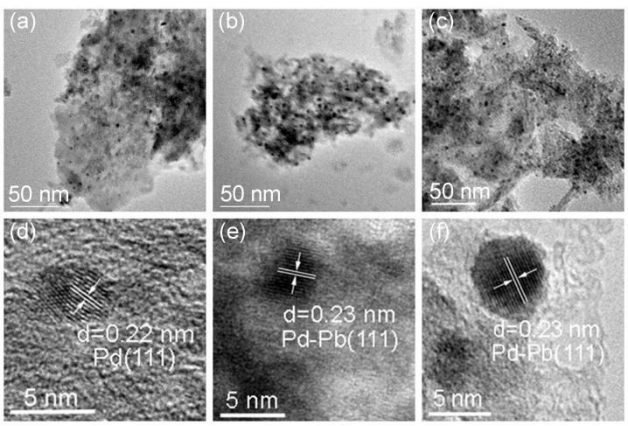

Fig. 2 TEM images of (a) Pd_2/Alumina, (b) Pd_2Pb_8/Alumina and (c) $Pd_5Pb_5Mg_2$/Alumina; HRTEM images of (d) Pd_2/Alumina, (e) Pd_2Pb_8/Alumina and (f) $Pd_5Pb_5Mg_2$/Alumina.

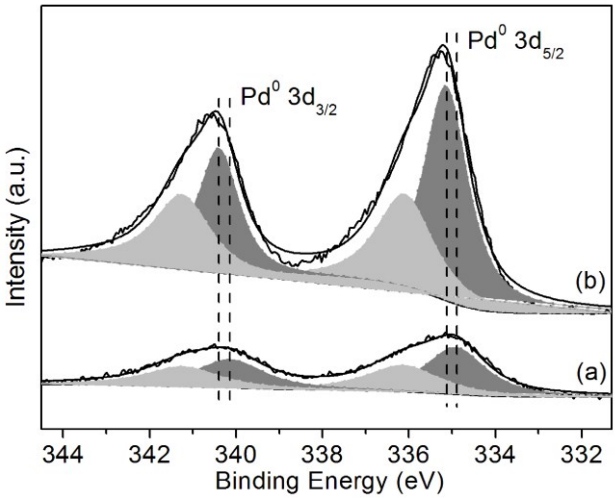

Fig. 3 XPS of Pd 3d for (a) Pd_2/Alumina and (b) Pd_2Pb_8/Alumina.

of Pd lattice after doping larger Pb atoms. HRTEM observations matched well with XRD measurements, both of which indicated that Pd-Pb bimetallic nanoparticles prepared with the novel and reported methods possessed the same Pd_3Pb structure. However, the particle size of Pd-Pb bimetallic nanoparticles is 4.4 nm for $Pd_5Pb_5Mg_2$/Alumina larger than 3.0 nm for that of Pd_2Pb_8/Alumina (Fig. 2 and S4). Corresponding Pd dispersion increased from 26 to 39%.[9] From the nano-scale viewpoint, pre-loaded Pb species facilitate to decrease the Pd-Pb bimetallic nanoparticle size, elevate the Pd dispersion and increase active site number. Wang and co-workers found that the oxidative coupling of methylacrolein with methanol is a structure-sensitive reaction and the catalytic efficiency increased with decreasing mean size of active nanoparticles.[4a] Therefore, Pd_2Pb_8/Alumina showed much higher catalytic efficiency than $Pd_5Pb_5Mg_2$/Alumina.

XPS was used to characterize the interaction of adjacent Pd and Pb atoms. The results were presented in Fig. 3. For Pd_2/Alumina catalyst, peaks with binding energies of 334.9 and 340.2 eV were assigned to Pd^0. For Pd_2Pb_8/Alumina catalyst, binding energies of Pd^0 3d$_{5/2}$ and 3d$_{3/2}$ appeared at 335.1 and 340.4 eV, respectively. Compared with monometallic Pd, binding energies shifted to higher positions after forming Pd-Pb bimetallic nanoparticles,[10] suggesting that Pb withdraw charge from adjacent palladium atoms and make the electrophilicity of palladium atoms increase.[11] Friend and co-workers illustrated that aerobic oxidative coupling of aldehydes with methanol started with deprotonation of methanol, the formed methoxy then attacked the aldehydic carbon atoms to form hemiacetal intermediates and further β-H elimination of hemiacetal released methyl esters.[1] Based on this oxidative coupling mechanism, electron-deficient palladium atoms promote the activation of aldehydes and facilitate the formation of hemiacetal intermediates. The β-H elimination of hemiacetal intermediates yields MMA.

Fig. 4 collects *in situ* FTIR spectra of adsorbed CO on Pd_2/Alumina and Pd_2Pb_8/Alumina. For the monometallic Pd_2/Alumina, CO was mainly adsorbed in the bridged mode at 1950 cm^{-1} with a small amount of CO adsorbed in linear mode. On the contrary, CO was mainly adsorbed in the linear mode at 2072 cm^{-1} on Pd_2Pb_8/Alumina. The reason could be attributed to the dilution effect of Pb to Pd, which inhibits the CO adsorption

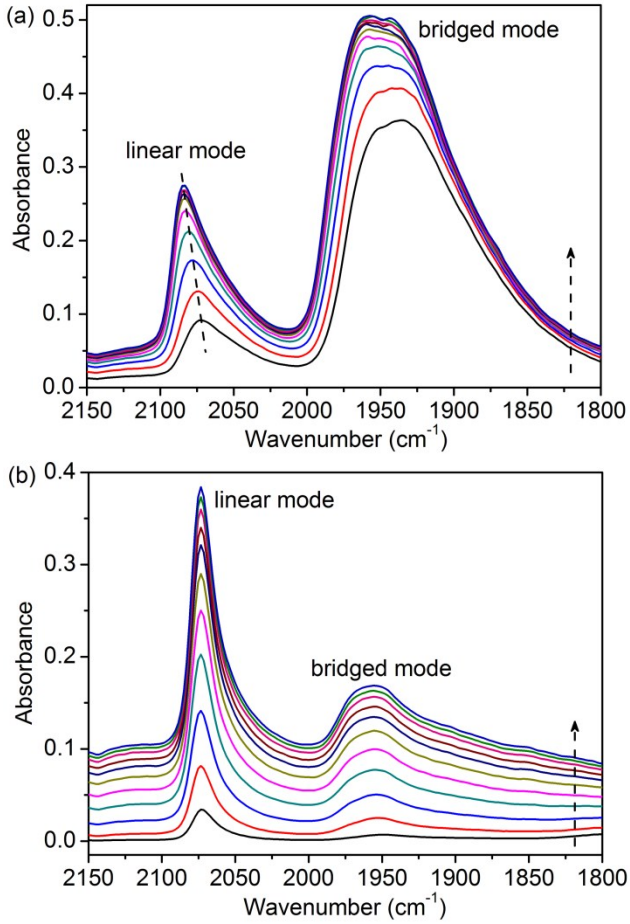

Fig. 4 *In situ* FTIR spectra of adsorbed CO on (a) Pd_2/Alumina and (b) Pd_2Pb_8/Alumina. The profiles for each sample were collected from 2 to 82 minutes (along the direction of arrow) with interval of 8 minutes.

on two Pd atoms (Fig. S5, ESI†). In addition, the frequency of linear-adsorbed CO on Pd_2/Alumina was blue shifted from 2072 to 2084 cm^{-1} with the increase of adsorption amount due to the interaction between the adsorbed CO molecules,[12] while almost no frequency shift was observed for linear-adsorbed CO on Pd_2Pb_8/Alumina, which further confirms the conclusion that Pb atoms dilute Pd clusters. There are similarities in the adsorbing mode between CO and aldehyde carbonyl groups (Fig. S5, ESI†). Hence, the dominant adsorbing mode of carbonyl alters from bridged to on-top mode after forming Pd-Pb bimetallic nanoparticles.[13] On one hand, the weakly on-top mode adsorbed carbonyls make side reactions such as decarbonylation, oxidation and hydrogenation more difficult to occur. On the other hand, the weakly on-top mode adsorbed carbonyls preserve the sp^2 hybridization form of the aldehydic carbon atoms, which possess low steric hindrance and facilitate the nucleophilic attack of the adsorbed methoxy intermediates.[14] Therefore, from the atom-scale viewpoint, the electronic interaction and the dilution effect of Pb to Pd inhibit side reactions and increase MMA selectivity.

When the oxidative coupling of methylacrolein was conducted with a methanol/aldehydes molar ratio of 16/1, a methylacrolein conversion of 96% with a MMA selectivity of 95% were obtained over Pd_2Pb_8/Alumina catalyst (Table 1, entry 13). Good to excellent conversion and selectivity were also achieved over Pd_2Pb_8/Alumina using isobutyraldehyde, benzaldehyde and

substituted benzaldehydes containing electron-donating and electron-withdrawing groups as the substrates (Table 1, entries 14-17), indicating that Pd_2Pb_8/Alumina catalyst showed a broad aldehyde range for the aerobic oxidative coupling reaction. We also found that after recycling for twenty times Pd_2Pb_8/Alumina catalyst still maintained high performance with the methylacrolein conversion of 70% and the MMA selectivity of 80% (Fig. S6, ESI†). The leaching of Pd was negligible after 22 recycles. Additionally, Pd_2Pb_8/Alumina catalyst was very robust. The particle size distribution profiles of alumina microspheres were very similar for fresh and used catalysts (Fig. S7 and S8, ESI†), indicating no obvious abrasion of alumina supporters occurred. In TEM images, no aggregation of Pd-Pb bimetallic nanoparticles was observed after 22 recycles (Fig. S9, ESI†). However, the particle size of Pd-Pb nanoparticles increased from initial 3.0 nm to 4.1 nm (Fig. S9, ESI†). The reason could be attributed to the Ostwald ripening, which is inevitable for liquid-participated reactions.

Conclusions

In conclusion, a highly efficient Pd_2Pb_8/Alumina catalyst for aerobic oxidative coupling of methylacrolein with methanol was prepared. The excellent performance of the novel catalyst was attributed to the multi-scale promoting effects of pre-loaded Pb species: (a) micron-scale, improving the formation of egg-shell structured active site distribution and providing more accessible active sites; (b) nano-scale, improving the dispersion of Pd precursors and increasing the active site number; (c) atom-scale, the electronic interaction and the dilution effect of Pb to Pd inhibited side reactions. As a result, the highest TON of 302 was achieved.

This work was financially supported by the National Key Basic Research Program of China (2015CB251401), the National Natural Science Foundation of China (21306203, 21127011) and Beijing Natural Science Foundation (2153042).

Notes and references

[a] *State Key Lab of Multiphase Complex System, CAS Key Lab of Green Process and Engineering, Beijing Key Lab of Ionic Liquids Clean Process, Institute of Process Engineering, Chinese Academy of Sciences, Beijing, 100190, China. Tel: 86-10-82544875; E-mail: sjzhang@ipe.ac.cn*

[b] *University of Chinese Academy of Sciences, Beijing, 100049, China.*

† Electronic Supplementary Information (ESI) available: Experimental details, supplementary tables and figures. See DOI: 10.1039/b000000x/

1 B.J. Xu, X.Y. Liu, J. Haubrich, R.J. Madix and C.M. Friend, *Nat. Chem.*, 2010, **2**, 61-65.

2 (*a*) S. Yamamatsu, T. Yamaguchi, K. Yokota, O. Nagano, M. Chono and A. Aoshima, *Catal. Surv. Asia*, 2010, **14**, 124-131; (*b*) Y. Mikami, A. Takeda and M. Oh-Kita, *US pat.*, 5 892 102, 1999.

3 (*a*) C. Liu, J. Wang, L.K. Meng, Y. Deng, Y. Li and A.W. Lei, *Angew. Chem. Int. Ed.*, 2011, **50**, 5144-5148; (*b*) B.H. Wang, W.J. Sun, J. Zhu, W.L. Ran and S. Chen, *Ind. Eng. Chem. Res.*, 2012, **51**, 15004-15010; (*c*) R.L. Oliveira, P.K. Kiyohara and L.M. Rossi, *Green Chem.*, 2009, **11**, 1366-1370.

4 (*a*) X.Y. Wan, W.P. Deng, Q.H. Zhang and Y. Wang, *Catal. Today*, 2014, **233**, 147-154; (*b*) J.X. Han, S.J. Zhang, J. Zhang and R.Y. Yan, *RSC Adv.*, 2014, **4**, 58769-58772; (*c*) S. Gowrisankar, H. Neuman and M. Beller, *Angew. Chem. Int. Ed.*, 2011, **50**, 5139-5143; (*d*) R.V. Jagadeesh, H. Junge, M.M. Pohl, J. Radnik, A. Bruckner and M. Beller, *J. Am. Chem. Soc.*, 2013, **135**, 10776-10782.

5 Y.Y. Diao, R.Y. Yan, S.J. Zhang, P. Yang, Z.X. Li, L. Wang and H.F. Dong, *J. Mol. Catal. A-Chem.*, 2009, **303**, 35-42.

6 (*a*) B.H. Wang, W.L. Ran, W.J. Sun and K. Wang, *Ind. Eng. Chem. Res.*, 2012, **51**, 3932-3938; (*b*) K. Suzuki, T. Yamaguchi, K. Matsushita, C. Iitsuka, J. Miuya, T. Akaogi and H. Ishida, *ACS Catal.*, 2013, **3**, 1845-1849.

7 F. Vratny and F. Gugliotta, *J. Inorg. Nucl. Chem.*, 1963, **25**, 1129-1132.

8 L.E. Alonso, K.P. de Jong and B.M. Weckhuysen, *Phys. Chem. Chem. Phys.*, 2010, **12**, 97-107.

9 W.H. Fang, J.S. Chen, Q.H. Zhang, W.P. Deng and Y. Wang, *Chem. Eur. J.*, 2011, **17**, 1247-1256.

10 (*a*) T.B.L.W. Marinelli and V. Ponec, *J. Catal.*, 1995, **156**, 51-59; (*b*) A.B. Anton, N.R. Avery, B.H. Toby and W.H. Weinbery, *J. Am. Chem. Soc.*, 1986, **108**, 684-694; (*c*) A.B. Anton, J.E. Parmeter and W.H. Weinbery, *J. Am. Chem. Soc.*, 1986, **108**, 1823-1833.

11 J. Goetz, M.A. Volpe, A.M. Sica, C.E. Gigola and R. Touroude, *J. Catal.*, 1997, **167**, 314-323.

12 B.T. Qiao, A.Q. Wang, X.F. Yang, L.F. Allard, Z. Jiang, Y.T. Cui, J.Y. Liu, J. Li and T. Zhang, *Nat. Chem.*, 2011, **3**, 634-641.

13 (*a*) J.L. Davis and M.A. Barteau, *J. Am. Chem. Soc.*, 1989, **111**, 1782-1792; (*b*) D.D. Garcia, I.F. Morales, F.J. Garzon, C.M. Castilla and M.P. Mendoza, *Langnuir*, 1999, **15**, 3226-3231.

14 J.L. Davis and M.A. Barteau, *Surf. Sci.*, 1992, **268**, 11-24.